Journal of Power Sources 196 (2011) 10201–10206

Contents lists available at SciVerse ScienceDirect

Journal of Power Sources

journal homepage: www.elsevier.com/locate/jpowsour

Synthesis of $LiNiO_2$ cathode materials with homogeneous Al doping at the atomic level

Zengcai Liu[a,*], Honghe Zhen[b], Yoongu Kim[c], Chengdu Liang[a,**]

[a] Center for Nanophase Materials Sciences, Oak Ridge National Laboratory, Oak Ridge, TN, 37831, United States
[b] School of Energy, Soochow University, Suzhou, 215000, PR China
[c] Materials Science & Technology Division, Oak Ridge National Laboratory, Oak Ridge, TN, 37831, United States

ARTICLE INFO

Article history:
Received 25 July 2011
Received in revised form 10 August 2011
Accepted 12 August 2011
Available online 22 August 2011

Keywords:
Raney nickel
Homogeneous doping
$LiNiO_2$
Lithium-ion batteries

ABSTRACT

Aluminum doped $LiNiO_2$ cathode materials are synthesized by using Raney nickel as the starting material. The structure and composition are characterized by X-ray diffraction (XRD) and scanning electron microscopy (SEM) coupled with elemental mapping. The lithium deficiency is analyzed by Rieveld refinement. The initial capacity and retention of capacity are correlated to the lithium deficiency of the resulting cathode material. Using strong oxidant of Li_2O_2 in the synthesis results in materials with improved electrochemical cyclability. The improvement is related to the diminishing of lithium deficiency in strong oxidizing synthesis conditions.

Published by Elsevier B.V.

1. Introduction

$LiNiO_2$ is considered as one of the promising cathode materials for lithium ion batteries because of its low cost, high energy density, and non-toxicity compared with $LiCoO_2$. However, it is difficult to synthesize $LiNiO_2$ with controlled composition and microstructure because of its tendency of cation mixing, resulting in nonstoichiometric $Li_{1-x}Ni_{1+x}O_2$ rather than stoichiometric $LiNiO_2$. The cation mixing is detrimental to the electrochemical performance of $LiNiO_2$. Low discharge capacity and poor cycling performance are always observed in $Li_{1-x}Ni_{1+x}O_2$ [1]. Moreover, thermal instability of highly deintercalated Li_xNiO_2 compounds could lead to severe safety problems [2].

Ohzuku et al. improved the electrochemical reactivity of $LiNiO_2$ by calcining the starting materials under pure oxygen [3]. $Li_{0.98}Ni_{1.02}O_2$, which is very close to stoichiometric one, is obtained from a mixture of Li_2O and NiO calcined at 700 °C under dry oxygen [4]. The instability of trivalent nickel ions at high temperatures and the presence of divalent nickel ions that situated at the lithium site lead to nonstoichiometric $Li_{1-x}Ni_{1+x}O_2$. $Li_{0.995}Ni_{1.005}O_2$ that was obtained by using three times excess lithium in the synthesis, demonstrated a large reversible capacity of more than 200 mA hg^{-1} that cycled at 3–4.5 V and 0.5 mA cm^{-2} [1]. Co substitution in $LiNiO_2$ tends to decrease the extra nickel ions at the lithium site and improves the structure stability and cyclability [5–9]. Al substitutions for nickel suppresses phase transitions during cycling, improves the thermal stability and the cyclability [2]. $LiNi_{1-y}Al_yO_2$ cathode materials synthesized from solid state method requires long heating times [2]. The resulting particles have inhomogeneous composition, irregular morphology, non-uniform particle size. Park et al. obtained $LiNi_{1-y}Al_yO_2$ using sol–gel method, and reported the improvement in cyclability at room temperature and 50 °C [10]. Guilmard et al. [11] synthesized $LiNi_{1-y}Al_yO_2$ using co-precipitation method with the aim to improve the compositional homogeneity. While cycling at 3–4.15 V, 0.05 C rate, the material showed improved cyclability. However, the capacity of the Al doped material decreases from 125 to 100 mA hg^{-1} when the doping level of Al amount increases from 10 to 25 at.%. Although the homogeneity of the starting material can be ensured by using solutions in the combustion method for the synthesis of Al doped $LiNiO_2$, not much improvements in discharge capacity and cyclability were observed in final materials [12]. Therefore, the homogeneity of the doping elements and the synthesis conditions are key to the electrochemical properties of $LiNiO_2$. In this sense, we explore a novel synthesis strategy to obtain homogeneous compositions of Al doped $LiNiO_2$ by using Raney nickel as the starting materials for Ni and Al. Raney nickel is obtained by selective dissolution of aluminum from NiAl alloy. The NiAl alloy is a homogeneous solid solution of metallic Ni and Al. Selective leaching of Al from the alloy results in a nanoporous material with homogeneous Al doped Ni framework. Since Ni and Al are homogeneously mixed in the

* Corresponding author. Tel.: +1 865 241 2409; fax: +1 865 574 1753.
** Corresponding author. Tel.: +1 865 574 8408, fax: +1 865 574 1753.
E-mail addresses: liuz@ornl.gov (Z. Liu), liangcn@ornl.gov (C. Liang).

0378-7753/$ – see front matter. Published by Elsevier B.V.
doi:10.1016/j.jpowsour.2011.08.059

starting materials, we expect to obtain homogeneous composition and single phase of $LiNi_{1-y}Al_yO_2$ with improved electrochemical performance.

2. Experimental

2.1. Synthesis of $Li_{1-x}Ni_{1+x-y}Al_yO_2$

$Li_{1-x}Ni_{1+x-y}Al_yO_2$ cathode materials were synthesized using Raney nickel and LiOH or Li_2O_2 as starting materials. Raney nickel, LiOH, $Ni(NO_3)_2$, $NH_3{\cdot}H_2O$ were purchased from Sigma. Raney nickel was deactivated by aqueous H_2O_2 solution prior to use. In a typical synthesis procedure, LiOH or Li_2O_2 was dissolved in a small amount of water and then impregnated into the deactivated Raney nickel. The Li to (Ni + Al) ratio was 1.1 and 0.6 for LiOH, 1.1 for Li_2O_2. The mixture was dried at 120 °C, and ground. The resultant mixture was precalcined at 600 °C and finally calcined at 750 °C for 20 h in a tube furnace under oxygen. LiOH or Li_2O_2 was melted and further impregnated into RND during the precalcination process. The resultant powder was washed with deionized water to remove impurities. The final products were dried at 120 °C. For comparison purpose, $LiNiO_2$ was prepared via a soft chemistry method [13]. Briefly, a basic solution of LiOH (1 M) and $NH_3{\cdot}H_2O$ (3 M) was added to a $Ni(NO_3)_2$ solution (1 M) under stirring with a Li to Ni ratio of 1.1. A gelatinous blue precipitate of $Ni(OH)_2$ was first obtained. Afterwards the mixture was slowly evaporated at 70 °C under primary vacuum in a rotary evaporator to remove the remaining water and ammonia. The recovered precipitate was dried at 110 °C and followed by calcination at 750 °C for 20 h in a tube furnace under oxygen. Compositions with corresponding synthesis conditions are summarized in Table 1.

2.2. Characterization of structure and composition

The powder X-ray diffraction (XRD) measurements were performed on a PANalytical Powder Diffractometer with a copper Kα (λ = 1.5416 Å) tube. The 2θ is scanned from 10 to 70° at a scan rate of 0.02° s^{-1}. Lattice parameters, lithium deficiency, and crystal size were obtained via Rietveld refinement analysis of the XRD patterns by using X'Pert HighScore Plus software. The morphologies of the powders were imaged on a Merlin SEM. The atomic compositions were analyzed by using an Inductively Coupled Plasma Optical Emission Spectrometers (ICP-OES).

2.3. Electrochemical measurements

Electrochemical measurements were conducted at a Maccor battery testing system by using Swagelok cells. The cathodes were prepared by slurry coating method with 80 wt.% of active material, 10 wt.% of Super S carbon black, and 10 wt.% of Polyvinylidene fluoride (PVDF, Sigma). Suitable amount of N-Methylpyrrolidone (NMP) was used as the dispersant. The slurry was prepared by mixing all ingredients with a homogenizer that spun at 3000 rpm for 15 min. The resultant slurry was applied onto carbon coated aluminum foil (Exopack Advanced Coatings, USA) using doctor blade. The solvent was dried overnight at 120 °C in a vacuum oven. Test cells ware assembled with a lithium metal anode and a Celgard 2325 separator in a glove box filled with argon. Commercial electrolyte of 1.2 M $LiPF_6$ in ethylene carbonate (EC)/diethyl carbonate (DEC) (v/v = 1:1) was used. All cells were cycled with constant current at about 0.05 C in the voltage range of 3.0–4.3 V.

3. Results and discussion

3.1. Deactivation of Raney nickel

Raney nickel is highly pyrophoric because of the adsorbed hydrogen that was generated from the leaching of Al from NiAl alloy in a concentrated alkaline solution [14]. The expose of dry porous sponge-like nickel framework leads to catastrophic combustion, which causes the loss of the porous structure. Therefore the deactivation/stabilization in H_2O_2 is a required step in this study [15]. Fig. 1 shows the XRD pattern and SEM image of Raney nickel after deactivation (RND). RND is composed of $Ni_{0.88}Al_{0.12}$ (43 at.%) and NiO (57 at.%) according to Rietveld refinement. Most likely NiO was resulting from the surface oxidation of Raney nickel from the deactivation step. The average crystal size is 7.8 and 3.3 nm for $Ni_{0.88}Al_{0.12}$ and NiO phases, respectively. However, ICP analysis (Table 1) shows that RND contains 74 at.% Ni and 26 at.% Al. The Al content obtained from ICP analysis is much higher than the values from XRD analysis. This discrepancy suggests the RND may contain certain amount of amorphous Al and/or Ni oxides. SEM image shows that the nanoporosity remained after deactivation. The porous structure facilitates the impregnation of LiOH. As expected, Al and Ni are uniformly distributed over the particles (Fig. 2).

3.2. Structural analysis and morphologies of $Li_{1-x}Ni_{1+x-y}Al_yO_2$

As a comparison, undoped $LiNiO_2$ (sample A) is synthesized via a soft chemistry method [11,13,16]. As shown in Fig. 3a (sample A), XRD pattern shows that $LiNiO_2$ has a 2D-$NaFeO_2$ type structure (*R*-3*m*). The (0 0 3) peak is from the diffraction of layered rock-salt structure, while the (1 0 4) peak appears from both the diffractions of layered and cubic rock-salt structures [17]. Ohzuku et al. [3] have correlated the integrated intensity ratio of (0 0 3) and (1 0 4) peaks ($I_{(003)}/I_{(104)}$) to the electrochemical reactivity: the electrochemically active $LiNiO_2$ has the $I_{(003)}/I_{(104)}$ greater than unity. As shown in Table 1, the $I_{(003)}/I_{(104)}$ of sample A is 1.13. This material is electrochemically active. The lattice parameters of *a* (2.877 Å) and *c* (14.19 Å) are very close to the reported values [3,4].

$Li_{1-x}Ni_{1+x-y}Al_yO_2$ was synthesized by impregnating RND with LiOH followed by calcining for 20 h at 750 °C in a tube furnace under O_2. The as-prepared sample (Fig. 3b, sample B) can be indexed to rhombohedral system (space group: *R*-3*m*), with a few minor impurity peaks. The impurities are Li_2O and Li_2CO_3, which can be removed by washing with deionized water (see Fig. 3b, sample B_W). The Li to (Ni + Al) ratio decreases from 1.30 to 1.08 after washing based on the ICP analysis. Washing with DI water also causes the decrease in peak intensities of the XRD patterns, although insignificant, washing out the impurities degrades the crystallinity of the material. Comparing with the undoped $LiNiO_2$, the (0 0 3) peak of sample B_W shifts to smaller 2θ and the lattice parameter *a* decreases. Given the difference of radius of cations, $r_{Al^{3+}}$ of 0.53 Å and $r_{Ni^{3+}}$ of 0.56 Å, the incorpation of Al^{3+} cations into the NiO_2 slab shifts the (0 0 3) peak and shrinks parameter *a* [18]. The large *c* parameter is caused by Ni^{2+} ($r_{Ni^{2+}}$ = 0.68 Å [18]) in the slab because of the insufficient oxidation of nickel in RND. The insufficient oxidation of nickel is probably due to the large particles of RND (Fig. 4a).

Sample C is a lithium deficient sample synthesized with nominal Li to (Ni + Al) ratio of 0.6 in the synthesis without considering the weight contribution of oxygen to RND (Fig. 3b, sample C). Rietveld refinement gives the composition of $Li_{1-0.15}Ni_{1+0.15-0.28}Al_{0.28}O_2$. With 15% of lithium deficiency, the lattice parameters of *a* and *c* increases to 2.8743 and 14.2398 Å. The increase of the Ni–Ni

Table 1
Composition and lattice parameters for RND and $Li_{1-x}Ni_{1+x-y}Al_yO_2$ cathode materials.

Samples	Starting materials		Li/(Ni + Al)		Lattice parameter		x	$I_{(003)}/I_{(104)}$
			Nominal	ICP	a	c		
RND				$Ni_{0.74}Al_{0.26}$				
A	$Ni(NO_3)_2$	LiOH	1.1	–	2.8770	14.1860	0.07	1.13
B	Raney nickel	LiOH	1.1	1.30	–	–	–	1.21
B_W	Raney nickel	LiOH	–	1.08	2.8702	14.1932	0.05	1.03
C	Raney nickel	LiOH	0.6	0.92	2.8743	14.2398	0.15	0.79
D	Raney nickel	Li_2O_2	1.1	1.41	–	–	–	1.17
D_W	Raney nickel	Li_2O_2	–	1.06	2.8763	14.2008	0.02	1.25

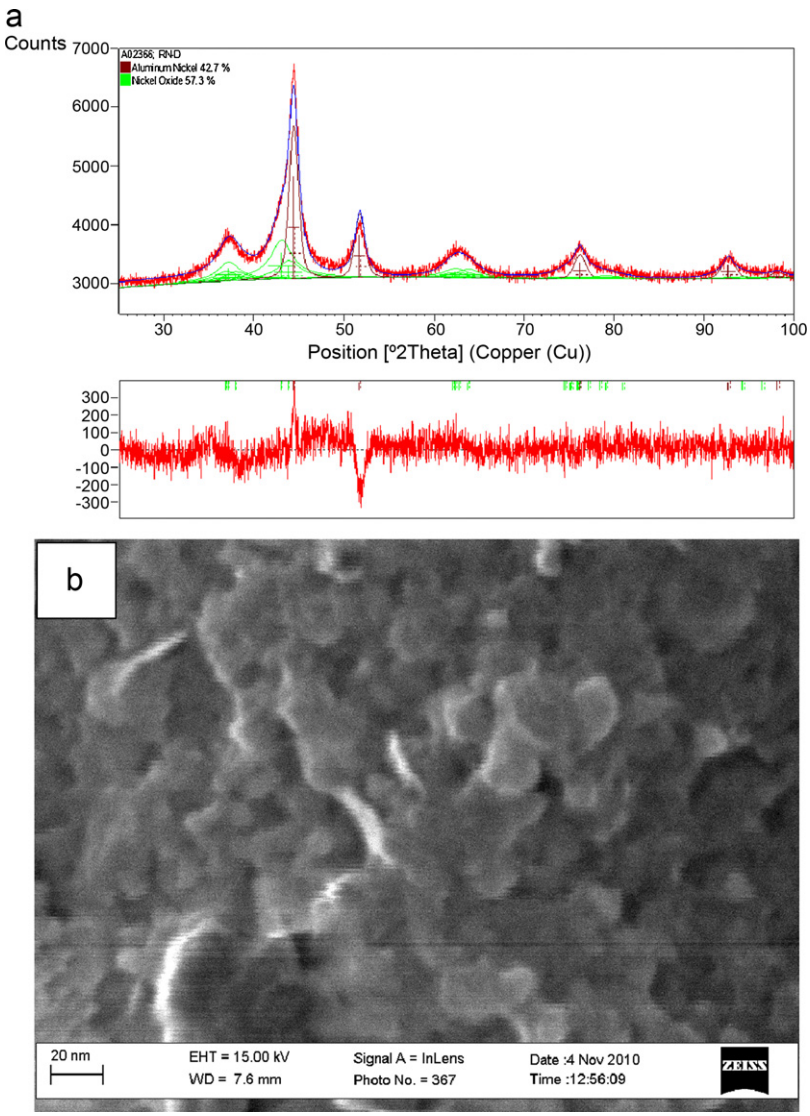

Fig. 1. XRD pattern and SEM image of deactivated Raney nickel.

distance (a) is attributed to the Ni^{2+} in the slab which is associated with the Li deficiency [4].

Replacing LiOH with Li_2O_2 in the synthesis, sample D_W is the least Li deficient sample with the x of 0.02 (Fig. 3b, sample D_W). This sampel has the highest ratio of $I_{(003)}/I_{(104)}$ among all samples. Apparently, using a strong oxidant in the synthesis reduces the cathion mixing in the final product.

There is no significant difference in the morphologies of all samples made from RND. The typical morphology of the samples is shown in Fig. 4b. The $Li_{1-x}Ni_{1+x-y}Al_yO_2$ particles inherit the morphology from RND. Water washing roughs the surface of the particles (Fig. 4c). This observation is consistent with the broadening of the XRD peaks after washing (Fig. 3b). There is no doubt that water washing could degrade the crystallinity of the particles.

3.3. Electrochemical activity

Fig. 5 shows the initial charge/discharge profiles between 3 and 4.3 V at 0.05 C (current: 22 mAg^{-1}). Sample A exhibits the highest initial charge capacity of 188 mAh g^{-1}, and discharge capacity of 143 mAh g^{-1}. The irreversible capacity loss of the first cycle is 45 mAh g^{-1}. This capacity loss is close to the reported values for

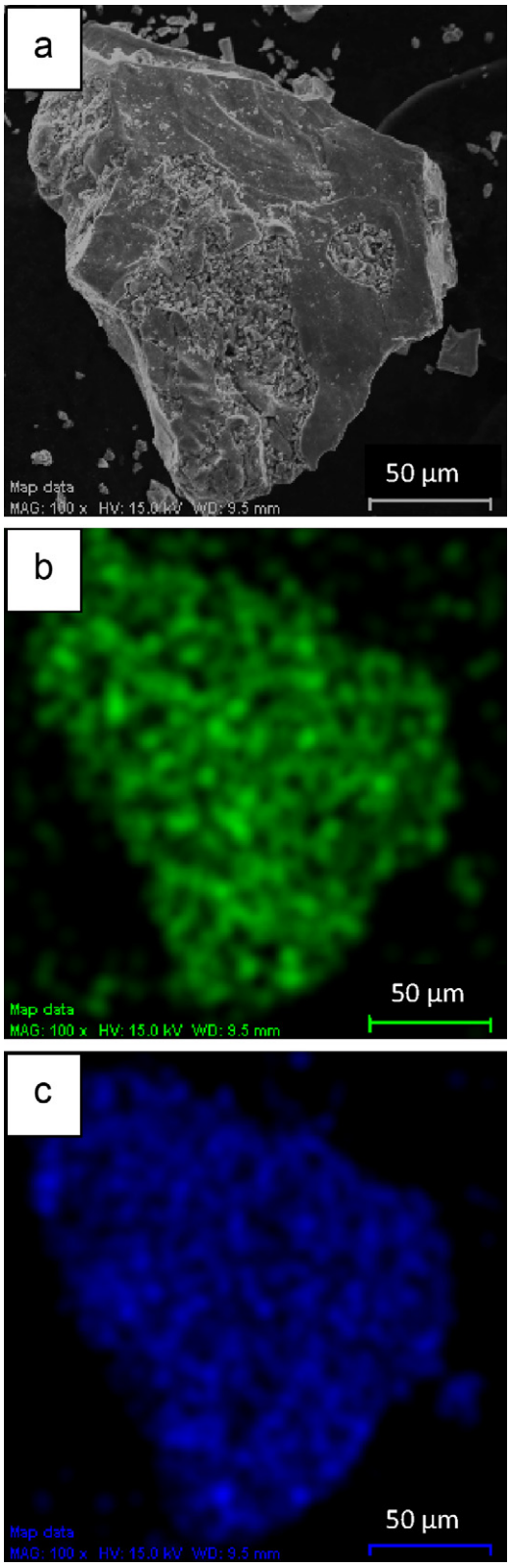

Fig. 2. SEM image (a) and elemental mapping (b) Al and (c) Ni of Raney nickel after deactivation.

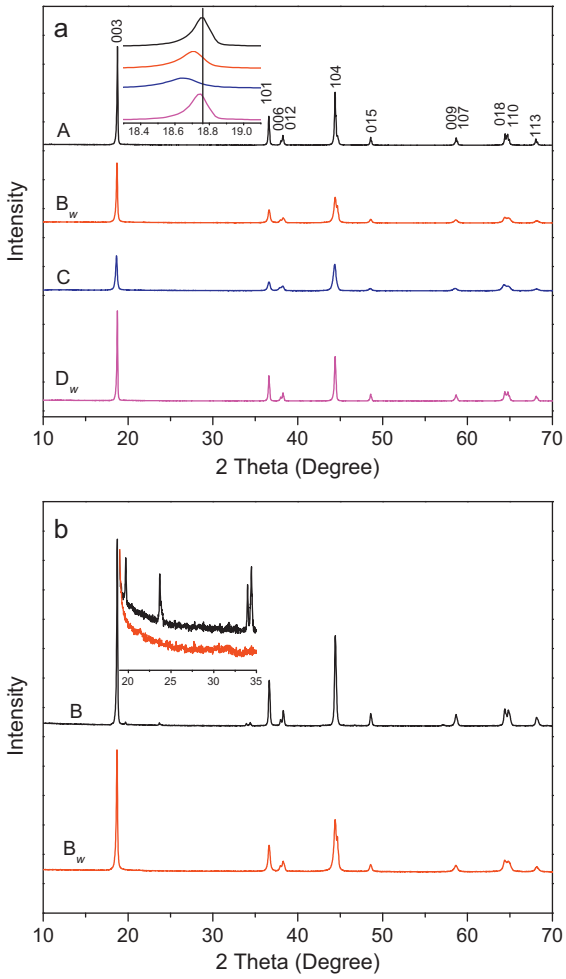

Fig. 3. XRD patterns of lithiated Raney nickel ($Li_{1-x}Ni_{1+x-y}Al_yO_2$). (a) Sample A, B_W, C and D_W, (b) sample B before and after washing.

the typical $LiNiO_2$ cathode materials [3,19,20]. The expansion of the interlayer distance during the charge deteriorates the layered structure leads to unrecoverable loss of capacity [3]. With Al doping, sample B_W gives slightly lower charge/discharge capacity due to the electrochemically inactive nature of Al. Similar capacity loss was observed in the first cycle. As expected, sample C, a lithium deficient sample has an initial charge/discharge capacity significantly lower than other samples. Large capacity loss of 53 mAh g^{-1} is observed. It is worth noting that although the sample D_W shows lower initial charge/discharge capacities than those of sample A and B_W, its irreversible capacity loss at the initial cycle is lower than all other samples.

The electrochemical cyclability is shown in Fig. 6. Sample A loses discharge capacity of 88 mAh g^{-1} over 20 cycles, corresponding to a fading rate of 4.4 mAh g^{-1} per cycle. The obvious capacity degradation is partially due to the high charging voltage of 4.3 V which is about 0.1 V higher than literature reported stable cycling voltage [3,11]. The high fading rate is due to the formation of NiO_2 at voltages above 4.2 V (vs Li/Li^+) [3]. The amorphous aluminum oxide after the deactivation of Raney nickel could be the possible cause of the rapid decay of capacity as well. In addition, the occupancy of lithium sites by the Ni^{2+} cations leads to the $Li_{1-x}Ni^{II}{}_x[Ni^{III}{}_{1-x}Ni^{II}{}_xO_2]$ formula that impedes the insertion and de-insertion of lithium ions [4]. High polarization is observed for the sample A with x of 0.07 during the discharging process (Fig. 6). When x increases, it is more difficult to reintercalate lithium. Doping with Al, sample B_W shows a slightly higher fading rate of

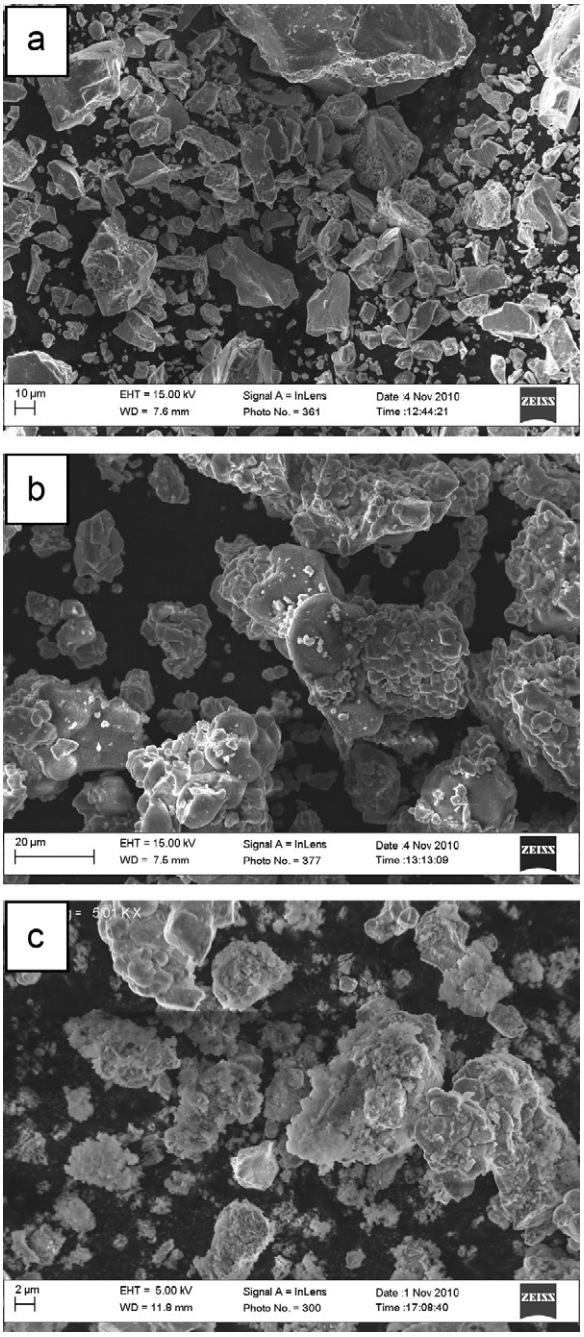

Fig. 4. SEM images of Raney nickel after deactivation (a), as-prepared sample B (b), sample B_W (c).

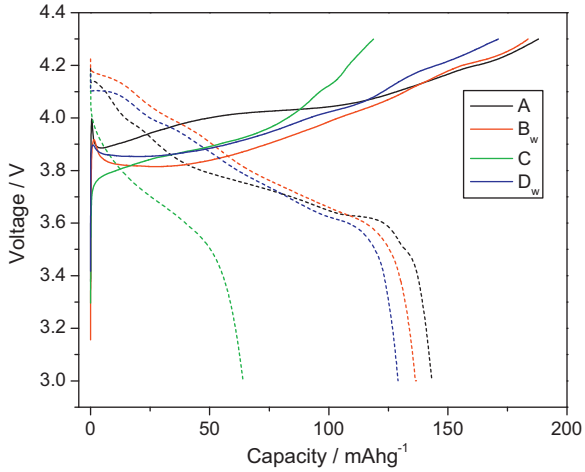

Fig. 5. Initial charge curve under constant current with cut-off voltage of 4.3 V and discharge curve under constant current with cut-off voltage of 3.0 V. Current: 5.5 mA g^{-1}, temperature: 25 °C.

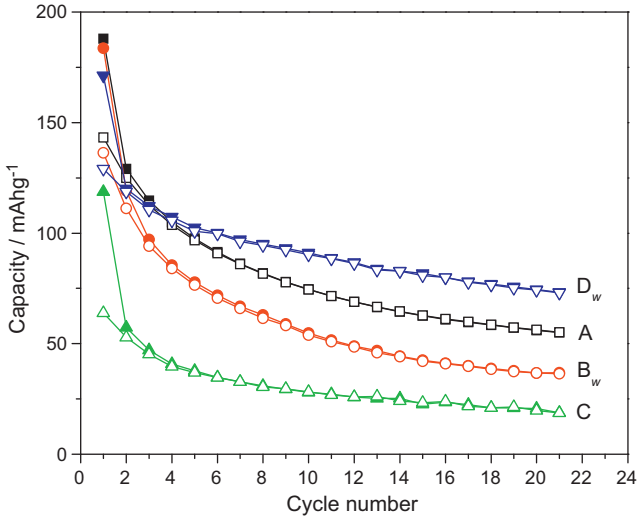

Fig. 6. Cyclability of $Li_{1-x}Ni_{1+x-y}Al_yO_2$ cathode between 3.0 and 4.3 V under constant current. Current: 5.5 mA g^{-1}, temperature: 25 °C.

5 mAh g^{-1} per cycle. The capacity fading is possibly due to the insufficient oxidation of nickel. Ohzuku et al. [3] attempted to synthesize $LiNiO_2$ with perfect structure using metallic nickel powder and LiOH as the starting materials, but failed to attain reproducible electrochemical testing results. In contrast to Ohzuku's results, samples prepared from RND are all electrochemically active with reproducible results. Raney nickel has a highly porous structure of sponge-like metallic framework. The porosity facilitates the access of lithium in the synthesis thus resulting materials with homogeneous composition and reproducible electrochemical properties. Rapid capacity decay was observed in the lithium deficient sample C. When stronger oxidant of Li_2O_2 is used during the synthesis, the sample D_W has a high discharge capacity of 73 mAh g^{-1} after 20 cycles. The fading rate of sample D_W is significantly lower than other samples. According to the XRD results, sample D_W has the least lithium deficiency. Appropriate oxidant used in the synthesis and homogeneous doping Al at atomic level minimize the cation mixing and lithium deficiency, thus stabilizing the crystal structure and improving the electrochemical cyclability of the $Li_{1-x}Ni_{1+x-y}Al_yO_2$ particles.

4. Conclusion

Electrochemical active $Li_{1-x}Ni_{1+x-y}Al_yO_2$ cathode materials were synthesized using Raney nickel as the source for nickel and aluminum which are homogeneously mixed at the atomic level. Highly porous structure of Raney nickel facilitates the access of lithium precursor to the metal framework and therefore leads to success in the preparation of electrochemically active samples with reproducible results. Strong oxidant of Li_2O_2 favors the formation of materials with less deficiency of lithium, consequently suppressing the cation mixing. The electrochemical cycling performance of the material with homogeneous Al doped sample and minimum lithium deficiency is superior to that of the materials without doping or with high level of lithium deficiency.

Acknowledgements

This work was sponsored by the Division of Materials Science and Engineering, Office of Basic Energy Sciences U.S. Department of Energy (DOE). The synthesis and characterization was conducted at the Center for Nanophase Materials Sciences, which is sponsored at Oak Ridge National Laboratory by the Division of Scientific User Facilities, U.S. DOE. The authors thank Dr Hongbin Bei for the discussion on the properties of Al–Ni alloys.

References

[1] H. Arai, S. Okada, H. Ohtsuka, M. Ichimura, J. Yamaki, Solid State Ionics 80 (1995) 261–269.
[2] T. Ohzuku, A. Ueda, M. Kouguchi, J. Electrochem. Soc. 142 (1995) 4033–4039.
[3] T. Ohzuku, A. Ueda, M. Nagayama, J. Electrochem. Soc. 140 (1993) 1862–1870.
[4] A. Rougier, P. Gravereau, C. Delmas, J. Electrochem. Soc. 143 (1996) 1168–1175.
[5] E. Zhecheva, R. Stoyanova, Solid State Ionics 66 (1993) 143–149.
[6] A. Rougier, I. Saadoune, P. Gravereau, P. Willmann, C. Delmas, Solid State Ionics 90 (1996) 83–90.
[7] H. Arai, S. Okada, Y. Sakurai, J. Yamaki, J. Electrochem. Soc. 144 (1997) 3117–3125.
[8] E. Levi, M.D. Levi, G. Salitra, D. Aurbach, R. Oesten, U. Heider, L. Heider, Solid State Ionics 126 (1999) 97–108.
[9] C. Delmas, I. Saadoune, Solid State Ionics 53 (1992) 370–375.
[10] S.H. Park, K.S. Park, Y.K. Sun, K.S. Nahm, Y.S. Lee, M. Yoshio, Electrochim. Acta 46 (2001) 1215–1222.
[11] M. Guilmard, A. Rougier, A. Grune, L. Croguennec, C. Delmas, J. Power Sources 115 (2003) 305–314.
[12] M.Y. Song, S.N. Kwon, S.D. Yoon, D.R. Mumm, J. Appl. Electrochem. 39 (2009) 807–814.
[13] V. Bianchi, D. Caurant, N. Baffier, C. Belhomme, E. Chappel, G. Chouteau, S. Bach, J.P. Pereira-Ramos, A. Sulpice, P. Wilmann, Solid State Ionics 140 (2001) 1–17.
[14] P. Fouilloux, Appl. Catal. 8 (1983) 1–42.
[15] M.A. Al-Saleh, R. Sleem Ur, S. Kareemuddin, A.S. Al-Zakri, J. Power Sources 72 (1998) 159–164.
[16] D. Caurant, N. Baffier, B. Garcia, J.P. Pereira-Ramos, Solid State Ionics 91 (1996) 45–54.
[17] J. Morales, C. Perezvicente, J.L. Tirado, Mater. Res. Bull. 25 (1990) 623–630.
[18] R.D. Shannon, C.T. Prewitt, Acta Crystallogr. B25 (1969) 925.
[19] S. Yamada, M. Fujiwara, M. Kanda, J. Power Sources 54 (1995) 209–213.
[20] Q.M. Zhong, U. Vonsacken, J. Power Sources 54 (1995) 221–223.